Physical and Engineering Sciences in Medicine
https://doi.org/10.1007/s13246-026-01726-2

SCIENTIFIC PAPER

Quantitative evaluation of radiotherapy accuracy in head and neck cancer: correcting cbct image distortions for improved tumour targeting and dose assessment

Reda Čerapaitė-Trušinskienė[1,3] · Diana Meilutytė-Lukauskienė[1,2] · Greta Karpavičienė[1,3] · Monika Jonušaitė[3] · Robertas Petrolis[1,4]

Received: 15 May 2025 / Accepted: 15 January 2026

Abstract

Image-guided radiotherapy (IGRT) has enhanced the precision of cancer treatment by integrating imaging modalities such as computed tomography (CT), magnetic resonance imaging (MRI) and cone-beam computed tomography (CBCT) into daily radiotherapy workflows. In head and neck cancer, where anatomical changes are common, accurate image registration between planning and treatment scans is essential to ensure dose accuracy. However, geometric distortions in CBCT (such as translation, rotation, and scaling resulting from patient positioning variations observed in daily CBCT images) can affect tumour targeting and dose delivery. This pilot study assesses a MATLAB-based image correction algorithm that uses rigid bony landmarks and point cloud registration together with spatial transformation to align CBCT with planning CT. Two head and neck cancer patients were retrospectively analysed, selected for their contrasting anatomical responses: one with substantial tumour regression and one with minimal change. Imaging was performed on the Halcyon V3.1 linear accelerator (Varian Medical Systems), with 25 daily CBCT scans per patient (85–96 slices per scan), resulting in 50 datasets for analysis. Spatial deviations were measured along the X, Y, and Z axes, and dose recalculations were performed for each treatment fraction. The correction method significantly improved spatial congruence and reduced geometric discrepancies caused by voxel spacing and acquisition parameters. Uncorrected scans showed dose deviations of up to ±12% in organs at risk, notably the spinal cord and parotid glands. These findings demonstrate the feasibility and dosimetric relevance of automated CBCT correction in daily head and neck radiotherapy. Although limited in sample size, the study provides a detailed technical and dosimetric analysis of spatial distortions and supports future validation in larger patient cohorts.

Keywords Cone-beam computed tomography (CBCT) · Spatial distortion · Adaptive radiotherapy (ART) · Head and neck cancer · Dose recalculation · Image registration

Introduction

Radiotherapy (RT) remains one of the most important modalities in cancer treatment, with its success highly dependent on technical precision and individualised planning. Over the past two decades, advances in engineering, imaging, and computational methods have led to the development of sophisticated radiotherapy techniques, such as image-guided radiotherapy (IGRT), intensity-modulated radiotherapy (IMRT) and stereotactic body radiotherapy (SBRT) [1, 2]. These approaches enable precise dose delivery to the target while sparing the surrounding healthy tissue, ultimately improving both tumour control and treatment

✉ Diana Meilutytė-Lukauskienė
diana.meilutyte-lukauskiene@lsmu.lt

1 Department of Physics, Mathematics and Biophysics, Lithuanian University of Health Sciences, Kaunas, Lithuania

2 Lithuanian Energy Institute, Kaunas, Lithuania

3 Radiotherapy Department of Hospital of Lithuanian, University of Health Sciences Kaunas Clinics Affiliate Hospital of Oncology, Kaunas, Lithuania

4 Lithuanian University of Health Sciences Neuroscience Institute, Kaunas, Lithuania

Published online: 11 March 2026

safety [3, 4]. As Gregoire et al. [2] emphasise, IGRT has become a cornerstone of precision in radiation oncology, enabling real-time tumour localisation and adaptive treatment strategies through high-resolution imaging.

Modern RT workflows increasingly depend on multimodality imaging strategies that integrate anatomical, functional and metabolic data to improve tumour delineation and adaptation during treatment. Computed tomography remains the standard for simulation and treatment planning due to its geometric accuracy [5], while magnetic resonance imaging (MRI) enhances soft tissue contrast and positron emission tomography (PET) provides valuable insights into metabolism activity [6–8]. These imaging modalities have also supported adaptive radiotherapy (ART), which allows real-time modification of treatment plans in response to tumour regression or anatomical changes during the course of treatment [9].

These needs are particularly acute in head and neck cancer (HNC), where tumour shrinkage, patient weight loss, and organ motion between fractions are frequent and clinically significant [10, 11]. The tumour microenvironment, including cancer-associated fibroblasts, immune cells, and the extracellular matrix, plays a key role in modulating radiosensitivity and contributes to differences in treatment response [10]. Biological factors such as tumour hypoxia, growth kinetics, and immune reactivation further complicate the radiobiological landscape of HNC and highlight the necessity for image-guided precision [11]. Cone beam computed tomography has become central to IGRT in HNC by enabling high-resolution volumetric imaging on treatment days [12, 13]. CBCT provides visual feedback for acute patient positioning and allows clinicians to monitor anatomical changes that can compromise dose delivery. Studies such as Guberina et al. [14] have shown that kV-CBCT-based ART allows narrower planning target volume (PTV) margins and more effective sparing of organs at risk (OARs), particularly in anatomically mobile regions such as the tongue and base of tongue. However, technical limitations remain. Similarly, Nath et al. [15] highlighted the advantages of IGRT for head and neck cancer, including improved tumour localisation, correction of interfractional variation, and adaptive replanning. However, there are still technical limitations. CBCT images often differ from planning CT scans in slice thickness, pixel pitch and field of view, leading to scaling, translation and rotation discrepancies [16, 17]. These distortions are particularly problematic in head and neck RT, where millimetre-level precision is critical to avoid overdosing structures such as the spinal cord, optic nerves, parotid glands or brainstem [18, 19]. Setup uncertainties also persist, even when rigid immobilisation with thermoplastic masks is used. As shown by Kang et al. [19], 2D and 3D image-guided registration techniques still leave residual translational and rotational errors, and a study by Alabedi [18] confirmed non-negligible PTV margin shifts in HNC patients despite imaging support. Previous studies, such as Yang et al. [20], have evaluated CBCT-based dose calculations and demonstrated their feasibility. However, motion artefacts and anatomical changes remain a challenge for accurate dose reconstruction in mobile sites such as the head and neck. More recently, Zhao et al. [21] demonstrated significant image quality improvements with ultrafast CBCT platforms, such as HyperSight, which offer enhanced Hounsfield Unit (HU) accuracy, scatter correction, and improved tumour delineation, further supporting the clinical value of advanced CBCT imaging.

To address these challenges, technological innovation is increasingly focussed on automation, consistency, and real-time adaptability. Fiorino et al. [1] emphasised the need for automated segmentation, plan creation and quality assurance, especially in resource-constrained environments. New CBCT platforms calibrated for accurate dose calculation (such as those evaluated by Bogowicz et al. [17]) have demonstrated improved imaging fidelity and CT number stability, supporting their use in adaptive planning. Volumetric guidance also enables a better understanding of motion management, particularly in the head and neck region where organ deformation and interfraction motion are common [13]. In addition, methodologies developed in MRI and PET imaging for distortion correction—such as prospective motion correction [22], data-driven motion correction [23], and field-map-based correction techniques [24], offer promising strategies that could be adapted to improve CBCT geometric accuracy. Patient-specific distortion correction [25] and digital reference object toolkits [26] further highlight the potential for enhanced image standardisation and target alignment.

Modern treatment platforms now offer integrated CT/MR imaging and real-time adaptive planning, emphasising the importance of accurate image registration and patient positioning [9, 27]. Despite the routine use of immobilisation devices such as thermoplastic masks or vacuum cushions, interfractional variations persist [28]. Although automatic image registration and adjustments made by the radiotherapy technician (RTT) usually take less than a minute [29], submillimetre deviations can still lead to clinically relevant deviations in dose delivery [30, 31]. Therefore, advanced computerised tools for image correction and distortion detection are essential to maintain treatment images. Quantitative image analysis supports the detection of distortions in CBCT data and improves anatomical alignment with planning CT geometry. Daily verification and correction mechanisms embedded in daily IGRT protocols will be crucial to enable adaptive, precise and individualised radiotherapy. As a pilot study, our aim is to evaluate

the feasibility and dosimetric implications of an automated correction pipeline using a limited yet extensive image dataset. The selected patient cases represent contrasting anatomical responses to treatment, allowing a comparative assessment of distortion patterns and correction robustness. In this pilot study, we evaluate the feasibility and dosimetric consequences of an automated kV-CBCT correction workflow, implemented using a MATLAB-based registration algorithm. The approach uses rigid alignment based on bony landmarks to quantify spatial deviations between planning CT and daily kV-CBCT datasets acquired on the Halcyon V3.1 platform. Head and neck cancer patients were retrospectively analysed, representing a range of anatomical responses to radiotherapy. The primary aim was to assess whether image registration-based correction improves geometric consistency and dose accuracy, particularly in patients with significant tumour regression. We hypothesise that residual spatial distortions in daily kV-CBCT imaging can compromise dose delivery to both target volumes and OARs, and that applying a rigid affine correction algorithm can mitigate these effects. Our results support the integration of automated image analysis into IGRT workflows, contributing to the advancement of adaptive and precision radiotherapy.

Methods

Data collection and study design

This retrospective pilot study analysed two patients with head and neck cancer who were selected because their tumours were well defined, the skull anatomy was clearly outlined, and patients were immobilised during treatment. The imaging data was provided by the Radiotherapy Department of the Hospital of Lithuanian University of Health Sciences (LUHS) Kaunas Clinics Affiliate Hospital of Oncology. To ensure patient confidentiality, all data sets were depersonalised prior to analysis. This retrospective study was conducted using data collected under ethical approval granted by LUHS Kaunas Clinics, permit No. [SPBT-68].

The first step in planning radiotherapy is to obtain a high-resolution computed tomography scan, which serves as a comprehensive anatomical reference (Fig. 1). This wide-angle image is essential for precise delineation of the clinical target volume (CTV), the planning target volume (PTV) and the neighbouring organs at risk (OARs). The resulting CT data set forms the geometric basis for creating an optimised treatment plan that delivers a therapeutic dose of radiation to the tumour while minimising exposure to surrounding healthy tissue. Treatment plans were created using the Eclipse Treatment Planning System (Varian Medical Systems) employing both intensity-modulated radiation therapy (IMRT) and volumetric modulated arc therapy (VMAT) techniques. Target volumes and OARs were delineated on the planning CT scans, following clinical contouring protocols. Dose constraints were applied in accordance with established international guidelines, including RTOG and QUANTEC. The prescribed dose for the initial phase of treatment was 50 Gy delivered in 25 fractions. Dose calculations were performed using the Anisotropic Analytical Algorithm (AAA) implemented within the treatment planning system. Figure 1 shows the high-resolution CT images acquired during the initial planning phase of radiotherapy. From left to right, axial, coronal and sagittal slices are shown with the CTV and PTV contours (in red), followed by a volumetric 3D representation of the patient's anatomy. These CT datasets allow precise delineation of tumour and OARs and serve as the basis for treatment dose calculation and daily image registration throughout radiotherapy.

During treatment, the patient's positioning is checked daily using the kilovoltage (kV) cone beam computed tomography (kV-CBCT) integrated into the linear accelerator. In contrast to planning CT, which provides a complete anatomical data set, kV-CBCT provides a more localised view, usually focusing on the PTV and its immediate surroundings (Fig. 2). This imaging approach minimises additional radiation exposure while providing sufficient detail for accurate repositioning of the patient. In the treatment of head and neck cancer, daily kV-CBCT scans allow physicians to detect anatomical changes and make daily positional adjustments before each fraction. As shown in Fig. 2, the image series shows the axial, coronal and sagittal kV-CBCT slices acquired just prior to treatment, along with a 3D representation of the patient's anatomy. These images are used to compare the current anatomy with the original planning CT to ensure alignment with the planned treatment geometry. Although essential for daily review, kV-CBCT presents some challenges: its limited field of view, increased

Fig. 1 Axial, coronal, sagittal, and 3D volumetric CT views of a glioblastoma patient for treatment planning

Fig. 2 Axial, coronal, sagittal kV-CBCT, and 3D volumetric views of a glioblastoma patient

Table 1 kV-CBCT imaging specifications of the halcyon V3.1 linear accelerator

Mode	11 protocols
Energy	80–140 kVp
Scan duration	From 16.6 s (for head, breast, chest modes) to 40.6 s (for large volume modes)
Scan range	24.5 cm
Scan diameter	49.1 cm
Imaging	17.5 cm lateral displacement limit
Pixel resolution	1280 × 1280 (43 × 43 active area)
Reconstruction	2 mm thickness
Reconstruction algorithm	Conventional CBCT, iterative process (iCBCT; non-linear/statistical)

Table 2 Residual post-RTT setup deviations based on CBCT-to-CT alignment across the X, Y and Z axes (patient with strong response to RT)

Coord.	Minimum, mm	Maximum, mm	Mean, mm	Std. Dev., mm
X	0.10	4.95	2.51	1.49
Y	0.10	4.40	2.13	1.31
Z	0.01	4.02	1.92	1.22

scattered radiation and variability in image resolution make it more susceptible to distortions such as translation, rotation and scaling errors. These factors must be considered when comparing daily kV-CBCT data with reference CT to ensure accurate dose delivery and consistent tumour targeting.

KV-CBCT collection and imaging characteristics

For this pilot analysis, two patients were retrospectively selected, each patient provided 25 daily kV-CBCT verification scans, resulting in 50 kV-CBCT datasets aligned against the planning CT. Each kV-CBCT set comprised between 85 and 96 axial slices. This high-volume temporal dataset allows for a detailed per-fraction analysis of spatial deviations and their cumulative dosimetric impact. Imaging was performed using the Halcyon V3.1 linear accelerator (Varian Medical Systems, Polo Alto, CA, USA) equipped with a kilovoltage cone-beam computed tomography system. The system includes a kV X-ray source with a semicircular titanium bowtie filter capable of generating tube voltages between 40 and 150 kV and an amorphous silicon detector with an active image active field of area of 43 cm × 43 cm (1280 × 1280 pixels). The kV-CBCT system supports 11 scan protocols tailored to the anatomical site and volume (Table 1). The use of a reconstruction thickness of 2 mm and iterative reconstruction algorithms (iCBCT) supports low-noise, high-contrast visualisation, which is crucial for accurate target localisation and deformable image registration. The combination of these specifications ensures the image consistency required for robust intra- and interfractional comparison.

Prior to treatment delivery, the patient was aligned to a virtual isocentre using external lasers, after which rigid 3D/3D image registration was performed between the kV-CBCT and planning CT. Couch shifts were then automatically applied in up to six degrees of freedom (6DoF). Importantly, even after correct couch correction, residual misalignments remain due to intrinsic CT–CBCT geometric differences. Identifying and quantifying these residual errors is the core objective of this study.

Nature of distortion in daily CBCT

A major challenge in the daily assessment of kV-CBCT images during radiotherapy is the occurrence of spatial distortions that affect image registration and treatment precision. These distortions associated with variations in patient positioning make it difficult to reliably compare the daily review scans with the original planning CT, which can lead to inaccurate tumour localisation and suboptimal dose delivery. The most common geometric discrepancies observed in kV-CBCT datasets include:

- Translational distortions—linear shifts in the spatial coordinates of anatomical structures typically caused by slight variations in patient positioning.
- Rotational distortions—angular deviations that occur during image acquisition and can cause anatomical structures to deviate from their expected orientation.
- Scaling distortions—inconsistencies in voxel size or image magnification, often due to mismatched acquisition parameters, leading to errors in volumetric analysis and tumour tracking.

Figure 3 presents examples of these distortions using a clinically realistic datasets from IAEA SHANE head and neck phantom. These simulated distortions reflect common

challenges encountered when comparing planning CT images with daily kV-CBCT scans, such as misalignment due to patient positioning or imaging protocol differences. The images illustrate how these distortions affect spatial alignment and highlight the importance of correction methods for accurate image registration during daily IGRT.

Combined, these distortions (translation, rotational and scaling) result in mislocalisation of bony reference structures, misalignment of tumour boundaries and OARs, degraded accuracy of deformable or rigid image registration, potential underdosage of the PTV or overdosing of sensitive structures. For these reasons, an effective correction method is needed to restore geometric congruence between CT and CBCT prior to dose evaluation.

Spatial transformation and correction process

To test our hypothesis, we conducted a comparative analysis using both uncorrected and post-corrected kV-CBCT datasets. The analysis included: (i) quantifying spatial deviations between corresponding anatomical landmarks in CT and kV-CBCT before and after correction, and (ii) recalculating radiation doses based on pre-corrected and post-corrected datasets to assess differences in target volume coverage and OAR exposure. The observed dosimetric discrepancies highlight the clinical importance of correcting kV-CBCT distortions to improve geometric accuracy. In three-dimensional (3D) medical imaging, geometric discrepancies such as translation, rotation and scaling often occur, which can distort the anatomical alignment between planning CT and daily kV-CBCT scans. These spatial transformations are modelled mathematically with 4×4 affine transformation matrix (T) that contains all three correction components:

$$T = \begin{pmatrix} a_{11} & a_{12} & a_{13} & a_{14} \\ a_{21} & a_{22} & a_{23} & a_{24} \\ a_{31} & a_{32} & a_{33} & a_{34} \\ 0 & 0 & 0 & 1 \end{pmatrix} \quad (1)$$

where the translation components (a_{14} - t_x, a_{24} - t_y, a_{34} - t_z) move the object in 3D space. Scaling components (a_{11} - s_x, a_{22} - s_y, a_{33} - s_z) adjust the object size along the coordinate axes. Rotation components are represented by individual rotation matrices (a_{22}, a_{23}, a_{32}, a_{33} - R_x; a_{11}, a_{13}, a_{31}, a_{33} - R_y; a_{11}, a_{12}, a_{21}, a_{22} - R_z), which are applied in sequence to correct angular displacements.

A translation matrix which is only moving an object along one or more of the three axes has this form:

$$T = \begin{pmatrix} 1 & 0 & 0 & t_x \\ 0 & 1 & 0 & t_y \\ 0 & 0 & 1 & t_z \\ 0 & 0 & 0 & 1 \end{pmatrix} \quad (2)$$

To apply a translation matrix to a point simply add the translation vector t_x, t_y, and t_z to the coordinates of a point (v_x, v_y, *and* v_z) producing translation (shift):

$$\begin{pmatrix} 1 & 0 & 0 & t_x \\ 0 & 1 & 0 & t_y \\ 0 & 0 & 1 & t_z \\ 0 & 0 & 0 & 1 \end{pmatrix} \begin{pmatrix} v_x \\ v_y \\ v_z \\ 1 \end{pmatrix} = \begin{pmatrix} v_x + t_x \\ v_y + t_y \\ v_z + t_z \\ 1 \end{pmatrix} \quad (3)$$

A spatial transform which changes the scale of an object by enlarging or reducing voxels or vertices along the axes by three scalar values specified in the matrix. A scaling matrix has this form:

$$T = \begin{pmatrix} s_x & 0 & 0 & 0 \\ 0 & s_y & 0 & 0 \\ 0 & 0 & s_z 0 & \\ 0 & 0 & 0 & 1 \end{pmatrix} \quad (4)$$

To apply a scaling transformation matrix to a voxel simply multiply it coordinates with the scaling values s_x, s_y, and s_z to the coordinates of it producing scaling factor:

$$\begin{pmatrix} s_x & 0 & 0 & 0 \\ 0 & s_y & 0 & 0 \\ 0 & 0 & s_z & 0 \\ 0 & 0 & 0 & 1 \end{pmatrix} \begin{pmatrix} v_x \\ v_y \\ v_z \\ 1 \end{pmatrix} = \begin{pmatrix} s_x \cdot v_x \\ s_y \cdot v_y \\ s_z \cdot v_z \\ 1 \end{pmatrix} \quad (5)$$

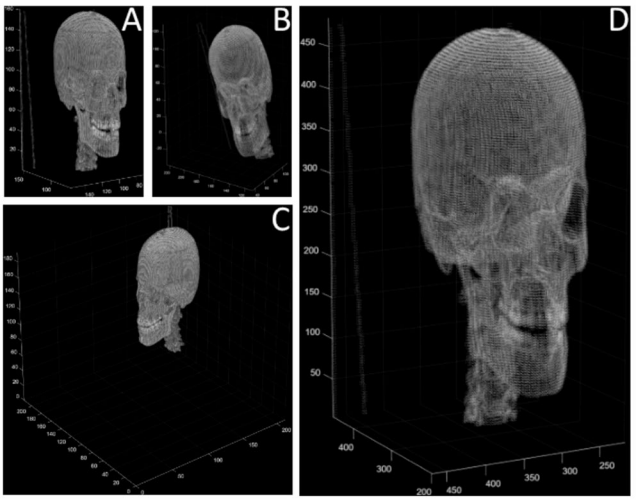

Fig. 3 Common types of geometric distortions in medical imaging during radiotherapy: **A** original CT image of the IAEA SHANE anthropomorphic head and neck phantom, **B** rotated image (angular distortion), **C** translated image (linear spatial shift), **D** scaled image (magnification distortion) D. All images were derived from CT datasets of the IAEA SHANE phantom

A rotation transformation matrix rotates an object about one of the three coordinate axes. If the object is rotated about two or more axes it is common to specify arbitrary rotations with a sequence of one-by-one axis rotations. In each case, the rotation is clockwise through an angle, about the given axis. The following three matrices R_X, R_Y and R_Z represent spatial transformations that rotate points through the angle θ:

$$R_x(\theta) = \begin{pmatrix} 1 & 0 & 0 & 0 \\ 0 & \cos(\theta) & \sin(\theta) & 0 \\ 0 & -\sin(\theta) & \cos(\theta) & 0 \\ 0 & 0 & 0 & 1 \end{pmatrix}$$

$$R_y(\theta) = \begin{pmatrix} \cos(\theta) & 0 & -\sin(\theta) & 0 \\ 0 & 1 & 0 & 0 \\ \sin(\theta) & 0 & \cos(\theta) & 0 \\ 0 & 0 & 0 & 1 \end{pmatrix} \quad (6)$$

$$R_z(\theta) = \begin{pmatrix} 0 & \cos(\theta) & \sin(\theta) & 0 \\ 0 & -\sin(\theta) & \cos(\theta) & 0 \\ 0 & 0 & 1 & 0 \\ 0 & 0 & 0 & 1 \end{pmatrix}.$$

To apply rotation transformation to a voxel simply multiply its coordinates with the specific rotation matrix in such order *x*, *y* or *z*.

Rotation matrices around each main axis (*X*, *Y*, *Z*) are applied in sequence to correct angular displacements. Each matrix rotates the coordinates by an angle θ around a specific axis. To correct these spatial distortions, a MATLAB-based image registration algorithm was implemented with the following workflow:

1. Generation of a sparse point cloud. High-density voxel regions, specifically bony anatomical landmarks, were extracted from both the daily kV-CBCT and planning CT datasets based on their HU intensity. These stable landmarks were used to create sparse 3D point clouds suitable for geometric registration. In our workflow, bony landmarks were identified automatically using a voxel intensity threshold of Hounsfield Units (HU) > 400, which corresponds to rigid skeletal structures. The segmentation focused on high-density anatomical regions, particularly the mandible and parts of the skull base, which demonstrate consistent visibility across both CT and kV-CBCT datasets. The resulting delineations were visually inspected in the initial test cases to confirm accurate identification of bony landmarks. Following this verification, the same thresholding procedure was applied uniformly across all kV-CBCT images for each patient. No manual annotations were introduced, ensuring full automation and reproducibility. A binary image mask was generated to isolate the bony anatomy voxels in the DICOM images. Each foreground voxel in this mask was treated as a 3D point (X, Y, Z), and the resulting set of points was used to construct the point cloud and perform the subsequent image-alignment procedures.
2. Iterative Closest Point (ICP) Matching workflow. The *pcregistericp* function in MATLAB was used to perform the alignment of the point clouds [32, 33]. Function was executed using the default *pcregistericp* settings, except these - "Metric" (correspondence metric) was set to "pointToPlane", "InlierRatio" was set to 0.8, extrapolation was enabled, "MaxIterations" was set to 60 and "Tolerance" (tolerance between consecutive ICP iterations - the algorithm stops when the average difference between estimated rigid transformations in the three most recent consecutive iterations is less than the specified tolerance values) was set to [0.00001, 0.001] ([Tdiff Rdiff], where Tdiff and Rdiff represent the tolerances of absolute difference in translation and in rotation, respectively, estimated in consecutive ICP iterations. Tdiff measures the Euclidean distance between two translation vectors. Rdiff measures the angular difference in degrees.). ICP iteratively minimises the distance between the moving (kV-CBCT) and fixed (CT) point sets by calculating the optimal affine transformation matrix. These settings ensured robust convergence while reducing the risk of overfitting to local noise or anatomical irregularities.
3. Application of the spatial transformation. The derived transformation matrix was applied to the kV-CBCT dataset using the *pctransform* function. This corrected translation, rotation and scaling distortions and aligned the image of the day with the reference geometry.

After correction, the spatially aligned kV-CBCT images were analysed to confirm anatomical congruence with the planning CT. This allowed for accurate tumour tracking and quantitative assessment of dose delivery. The distortions originate not from the kV-CBCT modality itself but from subsequent processing steps such as voxelization, interpolation, and alignment inaccuracies (associated to daily patient positioning).

Scaling distortions during image registration

One of the major challenges in daily radiotherapy imaging is the presence of scaling distortions caused by differences in image resolution and magnification between the initial planning CT and the subsequent daily kV-CBCT scans. These discrepancies are usually due to variations in the region of interest (ROI), scanner calibration or imaging protocol

settings. The significant differences in imaging parameters between the planning CT and daily kV-CBCT datasets are shown in Fig. 4. The planning CT scan (top row) was acquired with a slice thickness of 2.5 mm and a pixel pitch of 0.976562 × 0.976562 mm, ensuring a comprehensive anatomical reference for precise contouring of the CTV, PTV, and organs at risk. In contrast, the daily kV-CBCT scans (bottom row) used a finer slice thickness of ~ 1.99 mm and a smaller pixel pitch of 0.55 × 0.55 mm, with the field of view restricted to the PTV and adjacent structures. While this narrower imaging field limits unnecessary radiation exposure to the patient, it also leads to spatial inconsistencies that make image alignment and tumour tracking more difficult.

The consequences of scaling distortions in radiotherapy include.

1. Resolution discrepancies—variations in voxel size and slice thickness disrupt the geometric relationship between tumour boundaries and surrounding anatomy and affect consistency between different image sets.
2. Magnification effects—differences in image field size between CT and kV-CBCT result in misaligned anatomical landmarks and affect visual and computation registration.
3. Inaccurate registration—these inconsistencies can interfere with automatic or manual image fusion and may require deformable registration techniques to achieve spatial alignment.
4. Dosimetric effects—misregistration may result in under-dosing of the target or unintended irradiation of nearby critical structures, which may reduce the likelihood of tumour control and increase toxicity to normal tissue.

Recommendations to mitigate scaling errors: (1) standardisation of acquisition protocols—harmonisation of pixel pitch and slice thickness across CT and kV-CBCT platforms would minimise geometric discrepancies; (2) use of deformable image registration (DIR)—DIR methods can correct anatomical and geometric discrepancies by aligning volumes voxel by voxel, improving spatial consistency in image fusion; (3) Routine Quality Assurance (QA)—implementing systematic QA of image acquisition and registration workflows ensures early detection of resolution errors and maintains treatment accuracy.

Translational distortions due to errors in patient positioning

Translational distortions are caused by small but clinically relevant shifts in patient position between treatment fractions. Despite the use of immobilisation devices even submillimetre deviations in head and neck alignment can lead to misalignment between planning CT and daily kV-CBCT scans. These spatial inconsistencies affect the accuracy of tumour localisation and consequently the precision of dose delivery.

Translational discrepancies between the initial planning scan and follow-up kV-CBCT images reveal visible misalignments in the axial, coronal, and sagittal planes (Fig. 5).

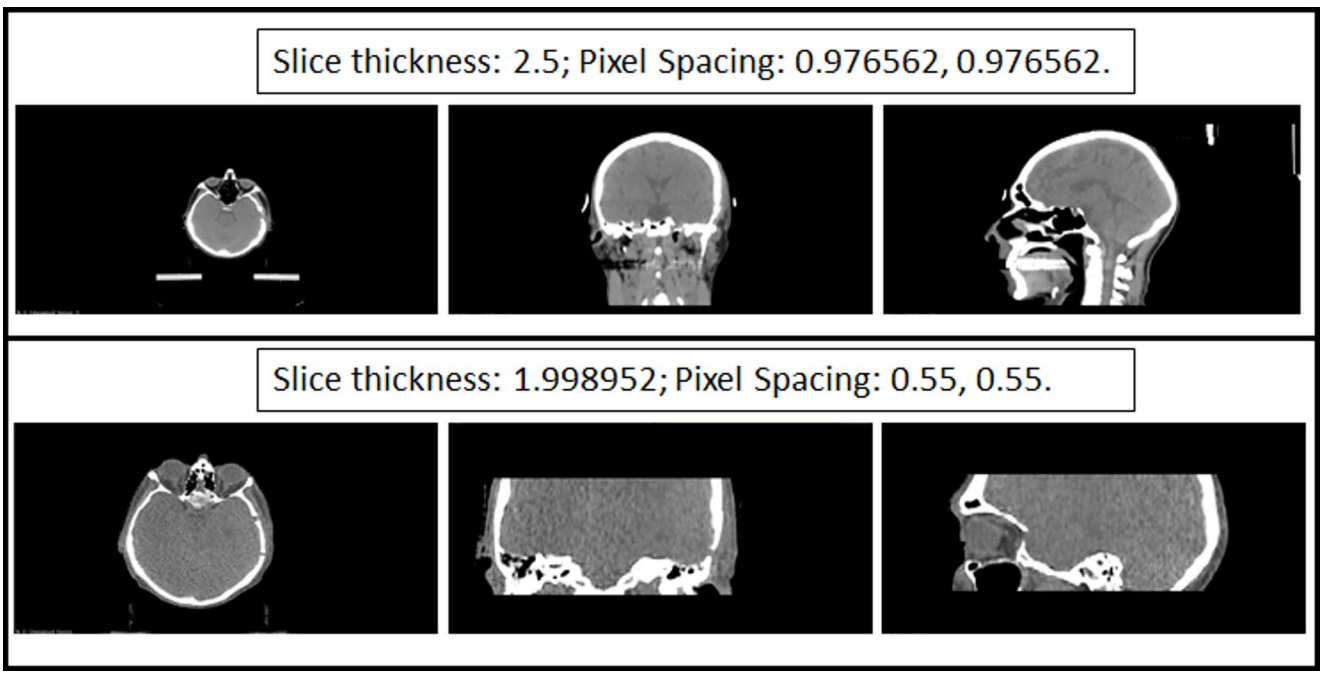

Fig. 4 Slides size difference between CT scan and daily kV-CBCT image

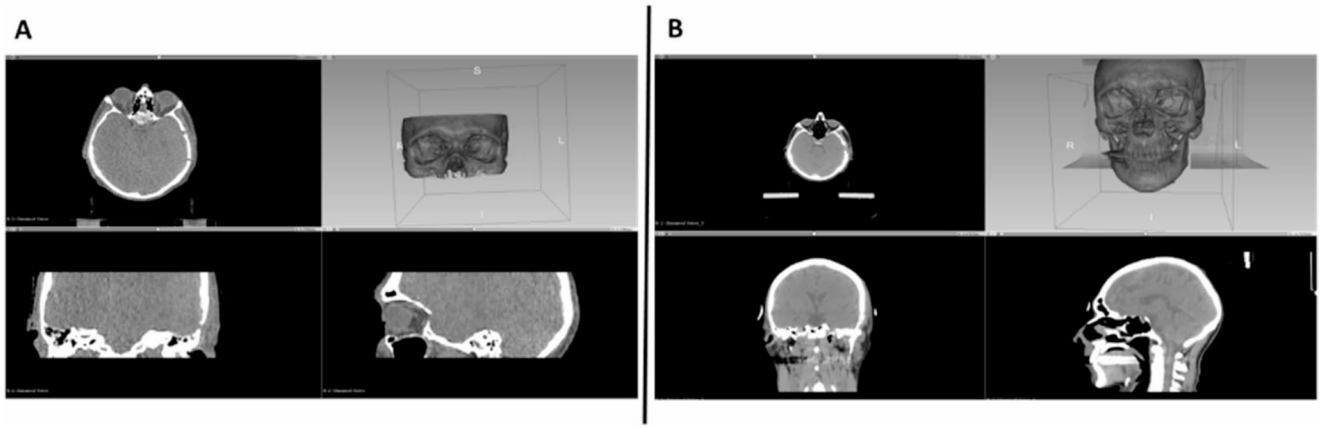

Fig. 5 Example of alignment discrepancies in kV-CBCT image sets for follow-up scans (**A**) and the initial planning scan (**B**)

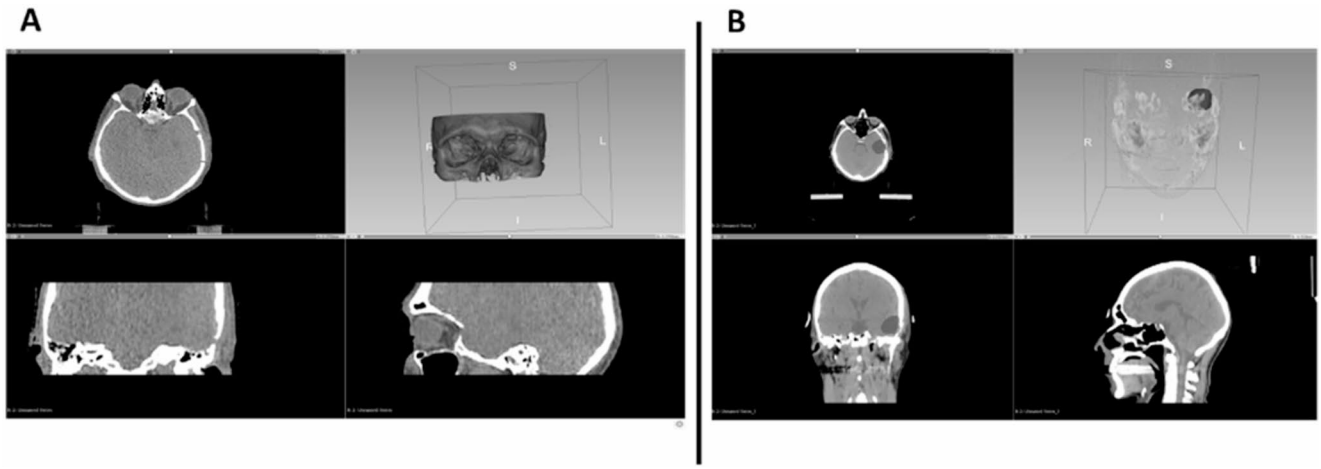

Fig. 6 Problems related to quantitative evaluation of daily (**A**) radiotherapy effectiveness due to the problematic nature of tumour (marked in **B**) volume detection from initial (**B**) kV-CBCT images

Figure 5B shows the initial planning scan, while Fig. 5A represents a follow-up scan during treatment. Clear differences in anatomical alignment are observed, indicating shifts in patient positioning over time. In addition to translational deviations, subtle rotational components (particularly evident in the axial view) further complicate image registration. 3D reconstructions illustrate these spatial inconsistencies, which may result in partial displacement of the CTV outside the high-dose region or unintended irradiation of OARs. If uncorrected, such geometric misalignments can compromise tumour localisation and reduce treatment accuracy.

The main consequences of translational bias include: (1) underdosing of the tumour: misaligned CTV and PTV may be partially outside the high dose range; (2) overdosing of healthy tissue: shifts in the patient's position can lead to unnecessary irradiation of OARs such as the spinal cord, parotid glands or brainstem; (3) uncertainty in image registration: translational errors degrade the spatial accuracy of multimodal image fusion and impair adaptive radiotherapy workflows. Meanwhile, strategies for correction are automated registration algorithms (feature- and intensity-based algorithms can detect and compensate for translational shifts based on anatomical landmarks or metrics of mutual information) and daily verification images (routine use of kV-CBCT facilitates early detection of misalignment and enables corrective action prior to dose delivery). This highlights the need for robust image registration tools and rigorous quality assurance protocols to minimise patient positioning errors and optimise clinical outcomes.

Rotational distortions in image registration

Rotational distortions refer to angular deviations between the daily kV-CBCT images and the original CT planning datasets. These deviations, which often occur in the axial, sagittal or coronal planes, can significantly affect the spatial accuracy of radiotherapy and lead to unintended dose distribution errors. Figure 6 shows a representative case of rotational deviation. The discrepancies between the

planning CT and subsequent kV-CBCT images illustrate how even subtle angular shifts can disrupt anatomical correspondence. The superimposed images show a problematic case of the tumour alignment in daily and initial kV-CBCT images, which poses a challenge for accurate image registration and dose calculation. Clinical effects of rotational errors/distortions include:

- Impaired target coverage: misaligned tumour volumes can lead to sub-optimal irradiation, resulting in underdosing of malignant tissue.
- Increased risk to organs at risk: angular deviations can shift high-dose regions towards sensitive anatomical structures, increasing the risk of radiation-induced toxicity.
- Heterogeneous dose distribution: rotational errors can lead to "hot spots" or "cold spots" within the dose field, which affects the uniformity of the treatment and the therapeutic outcome.

Strategies to correct rotation errors:

- Automated rotational registration: deformable image registration algorithms can correct angular misalignments by matching spatial features between kV-CBCT and CT images with high precision.
- Adaptive rotation monitoring: the integration of tracking systems enables early detection of rotational deviations so that corrections can be made before treatment fraction begins.
- Compensation of couch rotation: modern treatment couches support fine-tuning in multiple axes and enable physical correction of patient alignment in response to detected misalignments.

These results emphasise the critical role of advanced image registration and intrafraction verification technologies in maintaining geometric and dosimetric accuracy throughout radiotherapy.

Challenges in the quantitative assessment of radiotherapy outcomes

Accurate assessment of the effectiveness of radiotherapy requires consistent coordination between planning and subsequent imaging. However, daily imaging with cone beam computed tomography presents several challenges that can affect geometric and dosimetric accuracy. Discrepancies in field of view, voxel resolution and patient positioning between planning CT and daily kV-CBCT datasets can affect tumour localisation, especially when anatomical structures shift over time. Figure 7 illustrates the importance of accurate image registration. Unaligned datasets (panels A and C) show potential problems with image alignment like missing anatomical features (panel C) in the projections and region of interest selection (panel A), making quantitative tumour evaluation difficult. After applying affine correction,

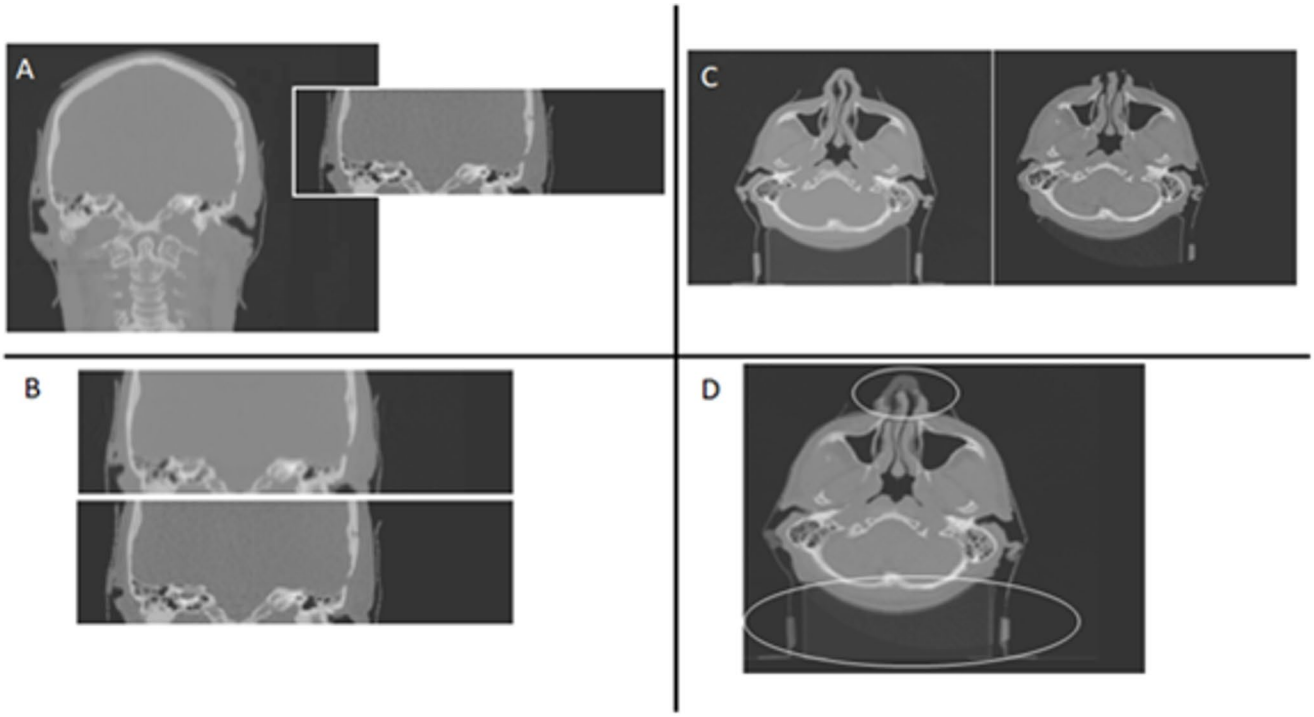

Fig. 7 CT and kV-CBCT images of different projections. Unaligned data sets **A** and **C**. Aligned data sets **B** and **D**

Table 3 Residual post-RTT setup deviations based on CBCT-to-CT alignment across the X, Y and Z axes (patient with a weaker response to RT treatment)

Coord.	Minimum, mm	Maximum, mm	Mean, mm	Std. Dev., mm
X	0.00	0.39	0.173	0.125
Y	0.00	0.39	0.142	0.122
Z	0.00	1.99	0.796	0.995

the aligned images (panels B and D) show improved spatial correspondence, emphasising the value of image correction algorithms to maintain anatomical accuracy and improve radiotherapy monitoring.

Results

To evaluate the consequences of CT–CBCT mismatch, we first quantified the residual positional deviations remaining after RTT couch corrections and then assessed their dosimetric impact.

Interfractional residual positional deviations

Residual spatial deviations between the planning CT and daily kV-CBCT were quantified after all clinically applied RTT couch corrections had been performed. These offsets represent the remaining CT–CBCT mismatch that persists despite correct clinical setup and therefore cannot be detected or eliminated through standard IGRT workflows alone. Tables 2 and 3 summarise the magnitude of these residual deviations along the X (lateral), Y (vertical), and Z (longitudinal) axes for the two patients included in this study. The patient with a strong anatomical response to radiotherapy exhibited substantially greater variability, with mean deviations ranging from 1.92 to 2.51 mm and maximum up to 4.95 mm. These values fall within the typical range of interfractional uncertainty reported for CBCT-guided head-and-neck radiotherapy; however, in this context, they represent residual rather than initial setup errors. In contrast, the second patient, who maintained relatively stable anatomy throughout treatment, showed minimal residual mismatch (mean deviations < 1 mm across all axes, maximum 1.99 mm). This highlights the strong influence of anatomical change on CT–CBCT geometric consistency, with tumour regression and soft-tissue shrinkage contributing to increased positional uncertainty even when immobilisation and IGRT guidance are used.

Table 4 Recalculated radiation doses for target structures and organs at risk based on observed patient positioning deviations (patient with a weaker response to RT treatment)

Structure	Planned dose, Gy	Minimum, Gy	Maximum, Gy	Mean, Gy	Std. Dev., Gy
CTV	49.21	49.05	49.26	49.1563	0.08052
PTV	43.46	41.89	44.24	43.065	1.17511
Parotid_L	25.03	23.85	26.35	25.0963	1.1311
Parotid_R	26.50	25.54	27.43	26.4838	0.84659
Spinal	46.03	46.15	46.3	46.2325	0.04683
Oesophagus	31.38	30.83	32.32	31.5525	0.60613
Larynx	32.47	32.13	32.87	32.4938	0.29895

Table 5 Percentage dose deviations from the planned values for endangered target structures and organs due to positioning errors (patient with a weaker response to RT treatment)

Structure	Planned dose, Gy	Minimum, %	Maximum, %	Mean, %	Std. Dev., %
CTV	49.21	-0.33	0.10	-0.11	0.164
PTV	43.46	-3.61	1.79	-0.91	2.704
Parotid_L	25.03	-4.71	5.27	0.26	4.519
Parotid_R	26.50	-3.62	3.51	-0.06	3.195
Spinal_Cord	46.03	0.26	0.59	0.44	0.102
Oesophagus	31.38	-1.75	3.00	0.55	1.932
Larynx	32.47	-1.05	1.23	0.07	0.921

Dosimetric impact of residual misalignments

To assess the clinical relevance of these residual deviations, dose distributions were recalculated by applying the measured CT–CBCT offsets to the original treatment plans. These recalculations estimate how residual misalignments affect the delivered dose to the PTV and organs at risk. For anatomically stable patients (Table 4), recalculated doses remained highly consistent with planned values. CTV and PTV variability were minimal (standard deviations 0.08–1.18 Gy), and all OAR doses remained within accepted tolerance levels. Percentage deviations (Table 5) were small for all structures, generally within ±1–2%. These results suggest that when anatomy is stable, residual CT–CBCT mismatch has little dosimetric consequence. In contrast, the patient with marked tumour regression exhibited substantially greater dose variability (Table 6). The spinal cord Dmax occasionally exceeded the clinically recommended QUANTEC limit of 45 Gy (maximum recalculated value: 45.51 Gy), indicating an increased risk of toxicity. The parotid gland showed variability up to ±1.72 Gy, and the oesophagus up to ±0.96 Gy. Larynx doses also fluctuated considerably (SD 2.47 Gy). When expressed as percentage deviations (Table 6), discrepancies were even more pronounced: Parotid_R ranged from −11.15% to +16.72%, Oesophagus from −12.91% to +12.21%, Spinal cord from −7.17% to +8.80%. Although the CTV and PTV remained

Table 6 Recalculated radiation doses for target structures and organs at risk based on observed patient positioning deviations (patient with a strong response to RT treatment)

Structure	Planned dose, Gy	Minimum dose, Gy	Maximum dose, Gy	Mean dose, Gy	Std. Dev. Gy
CTV	65.72	65.49	65.70	65.6088	0.09403
PTV	53.41	52.67	53.86	53.2913	0.39219
Parotid_R	18.12	16.10	21.15	18.7913	1.72440
Spinal Cord	41.83	38.83	45.51	41.9738	2.49011
Oesophagus	8.52	7.42	9.56	8.4738	0.95543
Larynx	39.71	36.95	42.44	39.7375	2.46972

Table 7 Percentage dose deviations from the planned values for endangered target structures and organs due to positioning errors (patient with a strong response to RT treatment)

Structure	Planned dose, Gy	Minimum, %	Maximum, %	Mean, %	Std. Dev. %
CTV	65.72	-0.35	-0.03	-0.1693	0.14307
PTV	53.41	-1.39	0.84	-0.2223	0.73430
Parotid_R	18.12	-11.15	16.72	3.7045	9.51656
Spinal_Cord	41.83	-7.17	8.80	0.3437	5.95292
Oesophagus	8.52	-12.91	12.21	-0.5428	11.21402
Larynx	39.71	-6.95	6.87	0.0693	6.21940

close to planned values, the magnitude of deviations in OARs demonstrates that even modest geometric mismatch can result in clinically meaningful dose errors, particularly in patients whose anatomy changes during treatment.

In summary, although both patients were treated with the same technology and treatment protocols, the clinical imaging results and dose accuracy differed significantly due to the different anatomical changes. For patients with stable structures, a CBCT-guided workflow may be sufficient. However, for patients with significant tumour regression, an adaptive radiotherapy approach (ART) that integrates image-based feedback and immediate plan changes is recommended. Routine geometric review, deformable image registration and stratified image review protocols should be considered as part of an adaptive clinical workflow to ensure treatment precision and optimise therapeutic outcomes. Taken together, these findings show that residual CT–CBCT misalignment is not negligible and can result in substantial dosimetric deviations. In patients with stable anatomy, these deviations remain small. However, in patients with dynamic anatomical changes, they can exceed commonly used clinical tolerance thresholds (e.g. parotid mean < 20–26 Gy, oesophagus mean < 34 Gy, spinal cord Dmax < 45 Gy). Such deviations may warrant repeated imaging, more frequent verification or mid-treatment replanning. These results underscore the need for improved correction methods, such as the ICP-based approach described in this study, to reduce residual geometric mismatch and thereby enhance the accuracy of CBCT-based dose assessment.

Discussions

This study demonstrates that even minor geometric discrepancies between planning CT and daily kV-CBCT datasets can result in measurable differences in dose delivery for head and neck cancer patients. Our analysis shows that spatial deviations (including translational, rotational, and scaling errors) persist despite the use of immobilisation devices and image-guided radiotherapy workflows. These findings are consistent with earlier reports highlighting the limitations of standard image-guided protocols in maintaining spatial and dosimetric accuracy [34, 35]. In patients with pronounced anatomical responses to treatment, our quantitative results showed average residual positional deviations between 1.92 and 2.51 mm in the patient with a strong anatomical response to RT (Table 2), consistent with Guberina et al. [14], who reported interfractional shifts of 2–3 mm in head and neck IGRT workflows. Importantly, these seemingly small discrepancies led to clinically meaningful dose deviations. Notably, recalculated spinal cord doses exceeded the maximum dose of 45 Gy (Table 6), surpassing the QUANTEC-recommended Dmax threshold associated with less than 1% risk of radiation-induced myelopathy [Marks et al., 2010]. Even a single treatment fraction with a higher dose may contribute disproportionally to toxicity, as subsequent fractions with lower doses cannot compensate for previous exceedances.

Similarly, the parotid gland and oesophagus received mean dose deviations of up to +16.72% and +12.21% respectively (Table 7), exceeding widely recognised constraints (e.g., parotid mean dose < 20 Gy for unilateral gland or < 26 Gy bilateral; oesophagus mean dose < 34 Gy). Although such deviations are not immediately life-threatening, they significantly increase the risk of xerostomia and Grade 3 or higher oesophagitis, both of which strongly affect patient quality of life. These findings suggest that when large geometric mismatches are visually apparent during daily verification, repeating the kV-CBCT after couch correction may be warranted. For patients with advanced tumours, mid-treatment replanning should be considered after evaluating geometric discrepancies and early dosimetric drift. Importantly, the comparison between uncorrected and post-corrected kV-CBCT-based dose calculations shows that residual geometric distortions directly cause dosimetric inaccuracies. Unprocessed kV-CBCT datasets produced OAR doses exceeding clinical tolerance thresholds (e.g., spinal cord Dmax > 45 Gy, parotid mean dose > 26 Gy). Although the affine correction algorithm does not improve

the treatment plan itself, it reduces these unintended deviations, indicating that geometric distortion correction can serve as a preventive safeguard within IGRT verification or adaptive workflows.

These dose variations were considerably less prominent in the patient with minimal anatomical change (Table 3), for whom the recalculated doses remained within acceptable limits (Tables 4 and 5). This contrast supports the findings of Enocson et al. [36], who demonstrated that daily ART with reduced margins preserved target coverage while significantly decreasing OAR doses (e.g., parotid reduction of 4.1 Gy). Together, these findings suggest that anatomically stable patients may be adequately managed with standard IGRT, whereas anatomically dynamic cases are more likely to benefit from ART protocols. Although the primary aim of this study was to evaluate kV-CBCT-based registration and correction, the results also highlight the clinical value of tracking anatomical changes during treatment. Patients with substantial tumour regression showed spatial shifts and OAR dose discrepancies. While identifying ART candidates was not an explicit objective, these findings suggest that image-based monitoring may prompt timely clinical review. For such patients, a multidisciplinary evaluation involving the radiation oncologist and medical physicist should be considered to determine whether replanning is necessary to maintain target coverage and OAR sparing. Lavrova et al. [37] similarly reported the increasing feasibility of CBCT-guided online ART workflows, while noting persistent limitations such as noise, scatter, and artefacts—factors we also observed as contributors to CT–CBCT alignment errors (Figs. 4, 5 and 6). Washio et al. [38] addressed this by evaluating iterative CBCT (iCBCT), which showed improved HU accuracy and gamma pass rates, suggesting that replacing conventional Feldkamp–Davis–Kress CBCT with iCBCT could enhance the reliability of daily dose recalculations. Moreover, Belotti et al. [16] and Poludniowski et al. [30] previously warned about anatomical variability and CBCT limitations, especially in OARs delineation. Our findings support these concerns: recalculated doses revealed OAR overdosing caused by geometric misalignment in kV-CBCT, particularly in deformable structures such as the oesophagus and parotids. As shown in Figs. 6 and 7, such geometric distortions substantially complicate reliable tumour localisation and OAR identification, underscoring the need to improve geometric fidelity in daily imaging.

Importantly, our implementation of a MATLAB-based volumetric alignment algorithm enabled identification and correction of rigid distortions. While not yet accounting for deformation or intrafractional motion, this method significantly improved consistency in anatomical localisation. Our work aligns with recent literature advocating automated correction tools to reduce inter-observer variability and enhance adaptive workflows [39, 40]. Integrating deformable registration (such as that employed by Enocson et al. [36]) and motion correction techniques from PET and MRI [22, 23] could further enhance this process. Nonetheless, this pilot study has several limitations. Most notable the small sample size ($n = 2$) restrict generalisability. However, the two cases represent contrasting anatomical responses, offering insight into the dosimetric implications of tumour dynamics. Furthermore, this study focused on interfractional misalignment errors, omitting interfractional motion and deformation variability, all factors known to affect dose [13, 41]. Future studies incorporating synthetic CTs, deformable registration, and larger patient cohorts are needed to validate and expand upon these findings.

In summary, this study highlights the significant impact of minor geometric misalignments in IGRT of the head and neck cancer. While standard workflows may be adequate for anatomically stable patients, dynamic cases require advanced image verification and adaptation strategies. Our findings support routine geometric review, dose recalculation, and the integration of automated correction tools to maintain treatment fidelity. As radiotherapy continues to progress towards real-time adaptive paradigms, strategies such as those described by Lavrova et al. [37], Washio et al. [38], and Enocson et al. [36] will be essential for improving precision and patient safety. Although our proposed correction algorithm substantially improves geometric alignment for rigid distortions, its effectiveness is reduced in cases of non-rigid deformation. This is particularly relevant when tumour volume shifts independently of the surrounding skeletal landmarks. For such patients, deformable registration algorithms that account for tissue deformation may be necessary to achieve accurate dose targeting. Future work should incorporate hybrid rigid–deformable workflows to address these anatomical variations more comprehensively.

Conclusions

This study illustrates the critical dosimetric and clinical consequences of seemingly minor residual geometric discrepancies in image-guided radiotherapy. Using daily kV-CBCT analysis and retrospective image registration, we identified and quantified spatial misalignments (specifically translational, rotational and scaling distortions) in head and neck cancer patients treated with CBCT-guided radiotherapy.

Positional misalignments ranged on average from 1.92 mm to 2.51 mm, with maximum shifts of almost 5 mm along the lateral axis. While the CTV and PTV coverage remained stable in most cases, the recalculated doses for the OARs showed considerable variability. The spinal cord, parotid glands and oesophagus were particularly susceptible

to unintended dose escalation, with variation of up to + 12%. In one case, the spinal cord exposure exceeded the standard limit of 45 Gy, emphasising the clinical risk of uncorrected misalignment.

Three important conclusions can be drawn from this analysis: (1) even millimetre-sized misalignments can have significant dosimetric effects, especially in anatomically dense regions such as the head and neck; (2) the routine use of daily kV-CBCT and advanced image registration algorithms is essential to detect and correct spatial distortions prior to dose delivery; (3) automated image processing techniques, such as the MATLAB-based alignment algorithm used here, provide a scalable, efficient tool to improve registration accuracy that supports both treatment-day decision making and retrospective treatment validation.

Incorporating such image correction techniques into clinical practice may increase treatment safety, reduce variability and provide the basis for wider adoption of adaptive radiotherapy. Further studies with larger patient cohorts are needed to validate this approach and assess its generalisability to different tumour types and anatomical sites.

This pilot study lays the groundwork for further multi-patient investigations by demonstrating the feasibility, precision, and clinical relevance of point-based kV-CBCT correction in head and neck radiotherapy.

Author contributions All authors contributed to the conception and design of the study. Greta Karpavičienė and Monika Jonušaitė were responsible for the image selection, the export of suitable images and the patient positioning data. Robertas Petrolis analysed the patient images, found structural discrepancies and compared them with the available positioning data to find discrepancies in patient positioning. Reda Čerapaitė-Trušinskienė recalculated the potential radiation doses based on the identified positioning discrepancies. Reda Čerapaitė-Trušinskienė and Diana Meilutytė-Lukauskienė revised and reviewed the final version of the article, discussed the results and contributed to the final manuscript.

Funding The authors declare that no funds, grants, or other support were received during the preparation of this manuscript.

Data availability Data can be available upon request to the authors.

Declarations

Conflict of interest The authors have no relevant financial or non-financial interests to disclose.

Ethical approval This study was approved by Lithuanian University of Health Sciences Kaunas Clinics and conducted as a retrospective analysis using previously collected data under permit No. [SPBT-68].

References

1. Fiorino G et al (2020) Quality of Care Standards in Inflammatory Bowel Diseases: a European Crohn's and Colitis Organisation. J Crohns Colitis 14(8):1037–1048. https://doi.org/10.1093/ecco-jcc/jjaa023
2. Grégoire V et al (2020) Image guidance in radiation therapy for better cure of cancer. Mol Oncol 14(7):1470–1491. https://doi.org/10.1002/1878-0261.12751
3. Garcia-Figueiras et al (2024) How imaging advances are defining the future of precision radiation therapy. Radio Graphics 44(2):e230152. https://doi.org/10.1148/rg.230152
4. Beaton L et al (2019) How rapid advances in imaging are defining the future of precision radiation oncology. Br J Cancer 120:779–790. https://doi.org/10.1038/s41416-019-0412-y
5. Metzger A et al (2019) Unforeseen computed tomography resimulation for initial radiation planning: associated factors and clinical impact. Adv Radiation Oncol 4(4):716–721. https://doi.org/10.1016/j.adro.2019.06.002
6. Martin O et al (2020) PET/MRI versus PET/CT for whole-body staging: results from a single-center observational study on 1,003 sequential examinations. J Nucl Med 61(8):1131–1136. https://doi.org/10.2967/jnumed.119.233940
7. Ohno Y et al (2016) Magnetic resonance imaging (MRI) and positron emission tomography (PET)/MRI for lung cancer staging. J Thorac Imaging 31(4):215–227. https://doi.org/10.1097/rti.0000000000000210
8. Wu M, Shu J (2018) Multimodal molecular imaging: current status and future directions. Contrast Media Mol Imaging 2018(1382183). https://doi.org/10.1155/2018/1382183
9. Sonke JJ et al (2019) Adaptive radiotherapy for anatomical changes. Semin Radiat Oncol 29(3):245–257. https://doi.org/10.1016/j.semradonc.2019.02.007
10. Peltanova B et al (2019) Effect of tumor microenvironment on pathogenesis of the head and neck squamous cell carcinoma: a systematic review. Mol Cancer 18(1):63. https://doi.org/10.1186/s12943-019-0983-5
11. Sminia P et al (2023) Clinical radiobiology for radiation oncology. In: Baatout S (ed) Radiobiology textbook. Springer, Cham. https://doi.org/10.1007/978-3-031-18810-7_5
12. Jaffray DA (2005) Emergent technologies for 3-dimensional image-guided radiation delivery. Semin Radiat Oncol 15(3):208–216. https://doi.org/10.1016/j.semradonc.2005.01.003
13. Korreman SS (2012) Motion in radiotherapy: photon therapy. Phys Med Biol 57:R161. https://doi.org/10.1088/0031-9155/57/23/R161
14. Guberina M et al (2024) Prospects for online adaptive radiation therapy (ART) for head and neck cancer. Radiat Oncol 19:4. https://doi.org/10.1186/s13014-023-02390-6
15. Nath SK et al (2009) Recent advances in image-guided radiotherapy for head and neck carcinoma. J Oncol 2009(1):752135. https://doi.org/10.1155/2009/752135
16. Belotti G et al (2023) Extension of the cone-beam CT field-of-view using two complementary short scans. Med Phys 54(5):3131–3818. https://doi.org/10.1002/mp.16869
17. Bogowicz M et al (2024) Evaluation of a cone-beam computed tomography system calibrated for accurate radiotherapy dose calculation. Phys Imaging Radiat Oncol 29:100566. https://doi.org/10.1016/j.phro.2024.100566
18. Alabedi H (2023) Assessing setup errors and shifting margins for planning target volume in head, neck, and breast cancer. J Med Life 16(3):394–398. https://doi.org/10.25122/jml-2022-0241
19. Kang H et al (2010) Accurate positioning for head and neck cancer patients using 2D and 3D image guidance. J Appl Clin Med Phys 12(1):3270. https://doi.org/10.1120/jacmp.v12i1.3270
20. Yang Y et al (2007) Evaluation of on-board kV cone beam CT (CBCT)-based dose calculation. Phys Med Biol 52:685. https://doi.org/10.1088/0031-9155/52/3/011
21. Zhao H et al (2025) Comprehensive image quality evaluation and motion phantom studies of an ultra-fast (6-second) cone-beam

computed tomography imaging system on a ring gantry linear accelerator. Adv Radiat Oncol 10(2):101681. https://doi.org/10.1016/j.adro.2024.101681
22. Sciarra A et al (2021) Quantitative evaluation of prospective motion correction in healthy subjects at 7T MRI. Magn Reson Med 87:646–657. https://doi.org/10.1002/mrm.28998
23. Spangler-Bickell MG et al (2022) Evaluation of data-driven rigid motion correction in clinical brain PET imaging. J Nucl Med 63(10):1604–1610. https://doi.org/10.2967/jnumed.121.263309
24. Gao Y et al (2021) Comparison and evaluation of distortion correction techniques on an MR-guided radiotherapy system. Med Phys 48(2):691–702. https://doi.org/10.1002/mp.14634
25. Dellios D et al (2021) Evaluation of patient-specific MR distortion correction schemes for improved target localization accuracy in SRS. Med Phys 48(4):1661–1672. https://doi.org/10.1002/mp.14615
26. Bae J et al (2024) Digital reference object toolkit of breast DCE MRI for quantitative evaluation of image reconstruction and analysis methods. Magn Reson Med 92:41728–1742. https://doi.org/10.1002/mrm.30152
27. Thörnqvist S et al (2016) Adaptive radiotherapy strategies for pelvic tumors—a systematic review of clinical implementations. Acta Oncol 55(8):943–958. https://doi.org/10.3109/0284186X.2016.1156738
28. Bujold A et al (2012) Image-guided radiotherapy: has it influenced patient outcomes? Semin Radiat Oncol 22(1):50–61. https://doi.org/10.1016/j.semradonc.2011.09.001
29. Coffey M, Leech M Introduction to the ESTRO European qualifications framework (EQF) 7 and 8: benchmarking radiation therapist (RTT) advanced education. Tech Innov Patient Support Radiat Oncol 8:19–21. https://doi.org/10.1016/j.tipsro.2018.09.008
30. Poludniowski GG et al (2012) Cone beam computed tomography number errors and consequences for radiotherapy planning: an investigation of correction methods. Int J Radiat Oncol*Biol*Phys 84(1):e109–e114. https://doi.org/10.1016/j.ijrobp.2012.02.019
31. Jassim H et al (2023) The geometric and dosimetric accuracy of kilovoltage cone beam computed tomography images for adaptive treatment: a systematic review. BJR|Open 5(1):20220062. https://doi.org/10.1259/bjro.20220062
32. Segal A, Haehnel D, Thrun S (2009) Generalized-ICP.In: Robotics: science and systems V, robotics: science and systems foundation. pp 435–442. https://doi.org/10.15607/RSS.2009.V.021
33. Korn M, Holzkothen M, Pauli J (2014) Color supported generalized-ICP. In: 2014 international conference on computer vision theory and applications (VISAPP). IEEE, pp 592–599. Lisbon, Portugal. https://doi.org/10.5220/0004692805920599
34. Rigaud B et al (2015) Evaluation of Deformable Image Registration Methods for Dose Monitoring in Head and Neck Radiotherapy. Biomed Res Int 2015(726268). https://doi.org/10.1155/2015/726268
35. Guckenberger et al (2012) Dosimetric consequences of translational and rotational errors in frame-less image-guided radiosurgery. Radiat Oncol 7:63. https://doi.org/10.1186/1748-717X-7-63
36. Enocson H et al (2025) Adaptive radiotherapy in locally advanced head and neck cancer: The importance of reduced margins. Phys Imaging Radiation Oncol 33:100696. https://doi.org/10.1016/j.phro.2025.100696
37. Lavrova E et al (2023) Adaptive radiation therapy: a review of CT-based techniques. Radiol Imaging Cancer 5(4):e230011. https://doi.org/10.1148/rycan.230011
38. Washio H et al (2021) Accuracy of dose calculation on iterative CBCT for head and neck radiotherapy. Phys Med 86:106–112. https://doi.org/10.1016/j.ejmp.2021.05.027
39. Hardcastle et al (2012) A multi-institution evaluation of deformable image registration algorithms for automatic organ delineation in adaptive head and neck radiotherapy. Radiat Oncol 7:90. https://doi.org/10.1186/1748-717X-7-90
40. Brouwer CL et al (2015) Identifying patients who may benefit from adaptive radiotherapy: Does the literature on anatomic and dosimetric changes in head and neck organs at risk during radiotherapy provide information to help? Radiother Oncol 115(3):285–294. https://doi.org/10.1016/j.radonc.2015.05.018
41. van Herk M (2004) Errors and margins in radiotherapy. Semin Radiat Oncol 14(1):52–64. https://doi.org/10.1053/j.semradonc.2003.10.003